Chapter 1 Introduction

The atmosphere is conventionally divided into layers based on the vertical structure of the temperature field. These layers, the troposphere, stratosphere, mesosphere, and thermosphere, are separated by the tropopause, the stratopause, and the mesopause (Fig. 1.1). In the past, meteorologists often designated the entire region above the tropopause as the "upper atmosphere." Only fairly recently has the term "middle atmosphere" become popular in referring to the region from the tropopause (10–16 km) to the homopause (at approximately 110 km). In this part of the atmosphere eddy processes keep the constituents well mixed and ionization plays only a minor role. It is this region of the atmosphere that is the concern of this volume. The upper atmosphere will here be defined as the region above the homopause, where molecular diffusion begins to dominate over eddy mixing so that constituents become separated vertically according to their molecular masses, and increased ionization makes electromagnetic forces significant in the dynamics. This distinction between the middle and upper atmospheres is now widely accepted, although the term "upper atmosphere" still appears fairly frequently in reference to the stratosphere and mesosphere. Thus, the *Upper Atmosphere Research Satellite* (*UARS*) is actually designed primarily for observation of the middle atmosphere. However, there can be little doubt that the name "middle atmosphere" will eventually become the standard term for describing the layers of the atmosphere between about 10 and 100 km.

1.1 The Static Structure of the Middle Atmosphere

Atmospheric statics is the study of the relationship among the thermodynamic variables pressure, density, and temperature (p, ρ, T). Given the

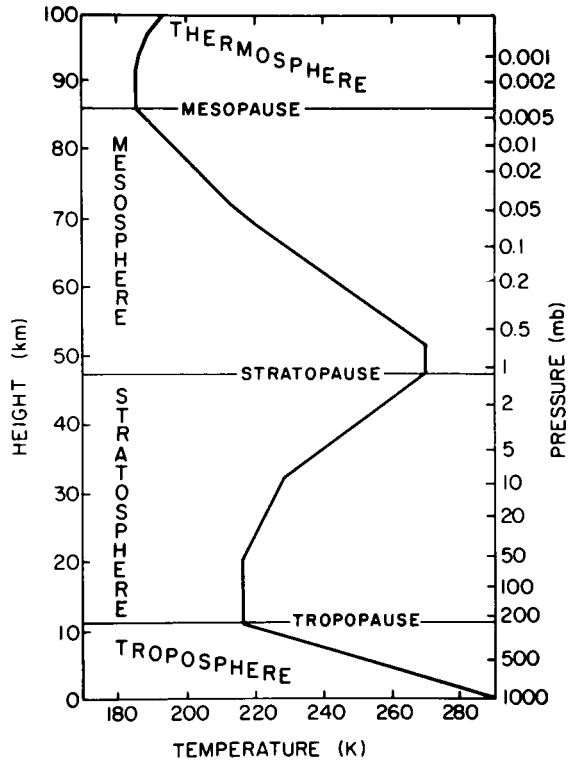

Fig. 1.1. Midlatitude temperature profile. Based on the *U.S. Standard Atmosphere* (1976).

vertical profile of temperature, the vertical profiles of pressure and density can be determined by use of the ideal gas law and the hydrostatic equation:

$$p = \rho RT, \tag{1.1.1}$$

$$\partial p/\partial z^* = -\rho g, \tag{1.1.2}$$

where R and g are the gas constant for dry air ($=287\ \mathrm{J\ K^{-1}\ kg^{-1}}$) and the magnitude of the gravity acceleration, respectively, and z^* is the geometric height.

1.1.1 The Hypsometric Equation

The geopotential is defined as the work required to raise a unit mass to height z^* from mean sea level:

$$\Phi \equiv \int_0^{z^*} g\, dz^*. \tag{1.1.3}$$

Using Eqs. (1.1.1)-(1.1.3) we can express the hydrostatic equation as

$$\partial\Phi/\partial \ln p = -RT, \tag{1.1.4}$$

which upon integration in p (with horizontal coordinates held constant) yields the *hypsometric* equation

$$Z_2 - Z_1 = \frac{R}{g_0}\int_{p_2}^{p_1} T\, d \ln p. \tag{1.1.5}$$

Here we have introduced the geopotential height Z defined by $Z \equiv \Phi/g_0$, where $g_0 = 9.80665\ \text{m s}^{-2}$ is the global average of gravity at mean sea level. As shown in Table 1.1, the difference between Z and z^* is negligible in the troposphere, but becomes increasingly significant in the upper mesosphere due to the decrease of g with height.

Table 1.1

The Relationship among Geometric Height z^*, Geopotential Height Z, Log-Pressure Height z, and Pressure p[a]

z^*	Z(km)	z(km)	p(mb)
0	0.00	−0.09	1.01325 + 3
10	9.98	9.30	2.6499 + 2
20	19.94	20.27	5.5293 + 1
30	29.86	30.98	1.1970 + 1
40	39.75	40.98	2.8714 + 0
50	49.61	49.94	7.9779 − 1
60	59.44	58.97	2.1958 − 1
70	69.24	69.02	5.2209 − 2
80	79.01	80.25	1.0524 − 2
90	88.74	92.46	1.8359 − 3
100	98.45	104.68	3.2011 − 4

[a] From *U.S. Standard Atmosphere* (1976). Note that 1 mb = 100 Pa. The integers in the far-right column (preceded by plus or minus signs) indicate the power of ten by which the particular entry should be multiplied.

The geopotential height difference $\Delta Z = Z_2 - Z_1$ between the pressure levels p_2 and p_1 is referred to as the *thickness* of the layer. If a layer mean temperature is defined as

$$\langle T(p_2, p_1)\rangle \equiv \left(\int_{p_2}^{p_1} T\, d \ln p\right) \Big/ \left(\int_{p_2}^{p_1} d \ln p\right). \tag{1.1.6}$$

then from Eq. (1.1.5)

$$Z = -[R\langle T(p, p_0)\rangle/g_0] \ln(p/p_0), \tag{1.1.7}$$

where p_0 is the pressure at $Z = 0$. Thus, in an isothermal atmosphere of temperature $\langle T \rangle$, pressure decreases exponentially with height by a factor of $1/e$ per scale height ($H \equiv R\langle T \rangle / g_0$).

If temperature varies with height, then Eq. (1.1.7) will only be valid if $\langle T \rangle$ is computed from Eq. (1.1.6) for each value of p. For this reason it is convenient to replace geopotential height by a log-pressure vertical coordinate defined by

$$z \equiv -H \ln(p/p_s), \tag{1.1.8}$$

where p_s is a standard reference pressure (usually taken as 1000 mb or 10^5 Pa)[1] and H is a mean scale height ($\equiv RT_s/g_0$, where T_s is a constant reference temperature). In middle atmosphere studies it is common to let $H = 7$ km, corresponding to $T_s \approx 240$ K. In that case, as shown in Table 1.1, for the U.S. Standard Atmosphere the difference between the geometric height and the log-pressure vertical coordinate defined in Eq. (1.1.8) is quite similar in magnitude to the difference between z^* and Z throughout the middle atmosphere, although for extreme temperature profiles (e.g., the polar night) the difference between z^* and Z can be substantially greater than shown in the table. Note also from Table 1.1 that z and Z both increase monotonically with z^*; this follows generally from their definitions and the hydrostatic relation of Eq. (1.1.2). In theoretical developments throughout this book we shall nearly always use z as the vertical coordinate and generally shall refer to z simply as "height"; we shall also use the symbol g in place of g_0, for convenience. Only for detailed comparisons with observations should it be necessary to distinguish among z^*, Z, and z, or to make allowance for the variation of g with height.

1.1.2 The Vertical Temperature Profile

A standard model for the mean midlatitude temperature profile is shown in Fig. 1.1. The mean vertical distribution of T in the middle atmosphere can be approximately explained in terms of absorption and emission of radiation. Infrared emission by water vapor and clouds is primarily responsible for the temperature minimum at the tropopause. The temperature peak at the stratopause is due to the absorption of solar ultraviolet radiation by ozone, and the minimum at the mesopause is primarily due to the large decrease in ozone concentration at that level, which greatly reduces the absorption of solar radiation.

[1] Throughout most of this book we shall use the millibar as the unit of pressure, in accordance with standard meteorological practice: 1 mb = 100 Pa.

1.1.3 Potential Temperature

The potential temperature θ is by definition the temperature that a parcel of dry air at pressure p and temperature T would acquire if it were expanded or compressed adiabatically to the reference pressure $p_s = 1000$ mb:

$$\theta \equiv T(p_s/p)^{\kappa} \tag{1.1.9a}$$

where $\kappa \equiv R/c_p \approx 2/7$ and c_p is the specific heat at constant pressure. Thus potential temperature, unlike temperature, is conserved for adiabatic flow. Because of this conservation property, θ is for some purposes superior to T as a field variable for characterizing the thermodynamic state of the atmosphere. Note that Eqs. (1.1.8) and (1.1.9a) imply

$$\theta = T \exp(\kappa z/H). \tag{1.1.9b}$$

From Eqs. (1.1.1), (1.1.2), and (1.1.9) it is easily verified that

$$T\,\partial \ln \theta/\partial z^* = g/c_p + \partial T/\partial z^*, \tag{1.1.10}$$

so that when the actual temperature *lapse rate*, $-\partial T/\partial z^*$, is less than the *adiabatic lapse rate*, g/c_p, potential temperature increases with height. The atmosphere is then said to be stably stratified or *statically stable*. The fact that potential temperature is a monotonically increasing function of height in a statically stable atmosphere means that θ can be used as an independent vertical coordinate. This "isentropic" coordinate system is discussed in Section 3.8.

1.1.4 Static Stability and the Buoyancy Frequency

The temperature profile of Fig. 1.1 indicates that the static stability in the stratosphere should be much greater than that of either the troposphere or the mesosphere. The most convenient measure of stability for dynamical studies is the square of the *buoyancy frequency*, which is the frequency of adiabatic oscillation for a fluid parcel displaced vertically from its equilibrium level in a stably stratified atmosphere (see, e.g., Holton, 1979, p. 50).

The buoyancy frequency squared, N_*^2, can be expressed in terms of potential temperature as

$$N_*^2 \equiv g\,\partial \ln \theta/\partial z^*. \tag{1.1.11}$$

In log-pressure coordinates a slightly modified "buoyancy frequency," defined as

$$N \equiv N_*(T/T_s), \tag{1.1.12}$$

proves to be the natural measure of stability (Gill, 1982, p. 184). From Eq. (1.1.8) with the aid of Eqs. (1.1.1) and (1.1.2) we find that $dz = (T_s/T)\,dz^*$,

so that

$$N^2 = g\left(\frac{T}{T_s}\right)\frac{\partial \ln \theta}{\partial z} = \frac{R}{H}\left[\frac{\partial T}{\partial z} + \frac{\kappa T}{H}\right]; \tag{1.1.13}$$

when $N^2 > 0$ the atmosphere is statically stable. In the stratosphere $N^2 \approx 5 \times 10^{-4}\,\mathrm{s}^{-2}$, while in the mesosphere $N^2 \approx 3 \times 10^{-4}\,\mathrm{s}^{-2}$. For analytic modeling it is often assumed that N^2 is constant throughout the middle atmosphere. However, it is important to realize that N^2 in the real atmosphere varies not only in the vertical but also with latitude, longitude, and season.

1.2 Zonal Mean Temperature and Wind Distributions

In the absence of eddy motions (i.e., departures from zonal symmetry) the middle atmosphere would be close to radiative equilibrium at all latitudes with a solstice temperature distribution similar to that shown in Fig. 1.2. Although the globally averaged temperature field at each altitude in the stratosphere and mesosphere is in approximate radiative equilibrium, eddy motions induce substantial local departures from equilibrium, especially in the winter stratosphere and near the mesopause in both winter and summer. The overall latitudinally dependent temperature distribution in the middle atmosphere arises from a balance between the net radiative drive (i.e., the sum of the solar heating and infrared heating or cooling) and the heat transport plus local temperature change (often called the dynamical heating or cooling) produced by these motions.

The net radiative heating distribution has a strong seasonal dependence, with maximum heating at the summer pole and maximum cooling at the winter pole. At the equinoxes the maximum heating is at the equator and there is cooling at both poles. The circulation in the meridional plane that dynamically balances this differential heating is often called the *diabatic circulation.* However, as discussed in Chapter 7, this circulation is primarily driven by eddy forcing, not by radiative heating directly. At the solstices the diabatic circulation consists of rising motion near the summer pole, a meridional drift into the winter hemisphere, and sinking near the winter pole. The Coriolis torque exerted by this meridional drift tends to generate mean zonal westerlies in the winter hemisphere and easterlies in the summer hemisphere that are in approximate geostrophic balance with the meridional pressure gradient. At the equinoxes the differential radiative drive is associated with a fairly weak diabatic circulation, with rising in the equatorial region and a poleward meridional drift in both the spring and autumn

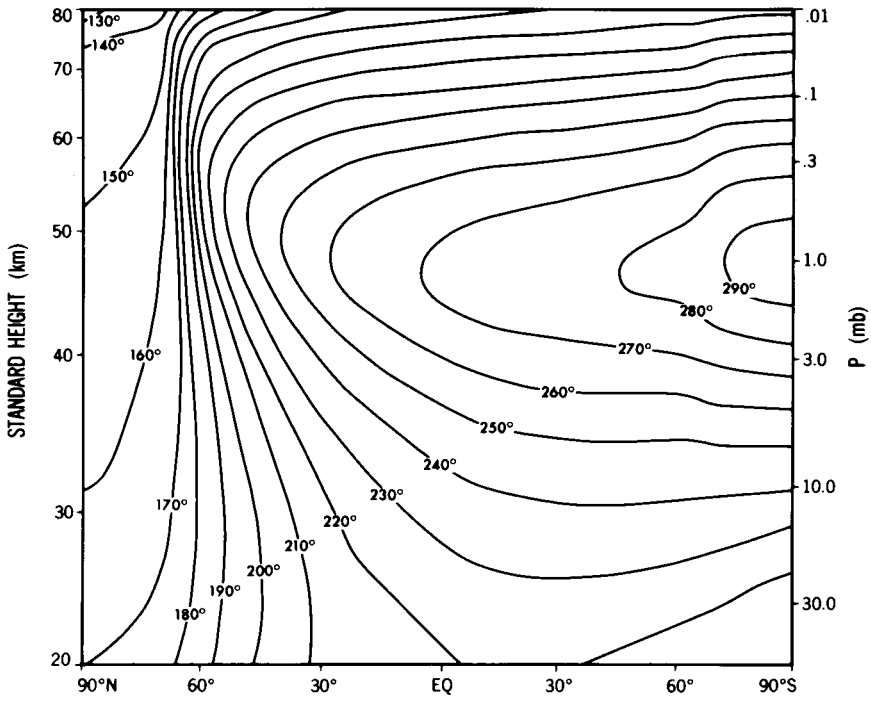

Fig. 1.2. Time-dependent "radiatively determined" temperature T_r for January 15 from a radiative-convective-photochemical model that is time-marched through an annual cycle. The surface temperatures are prescribed at their seasonally varying observed zonal mean values, and the tropospheric lapse rate is specified at 6.5 K km^{-1}. Cloudiness and the ozone below 25 km are prescribed at annual mean values; ozone above 25 km is computed by a detailed photochemical model. [From Fels (1985).]

hemispheres. The Coriolis torque thus generates weak mean zonal westerlies in both hemispheres.

Schematic cross sections of the longitudinally averaged solstice mean temperature and zonal wind fields for the middle atmosphere are shown in Figs. 1.3 and 1.4, respectively. The zonal mean wind is in approximate thermal wind balance with the temperature field, so that the vertical wind shear is proportional to the meridional temperature gradient, as can be qualitatively confirmed from the figures. Although the rather uniform increase of temperature from the winter pole to the summer pole in the region of 30–60 km is consistent with the radiative equilibrium distribution of Fig. 1.2, there are a number of features of the climatological temperature distribution that are not even qualitatively in accord with the distribution of radiative sources and sinks. These include the temperature increase in

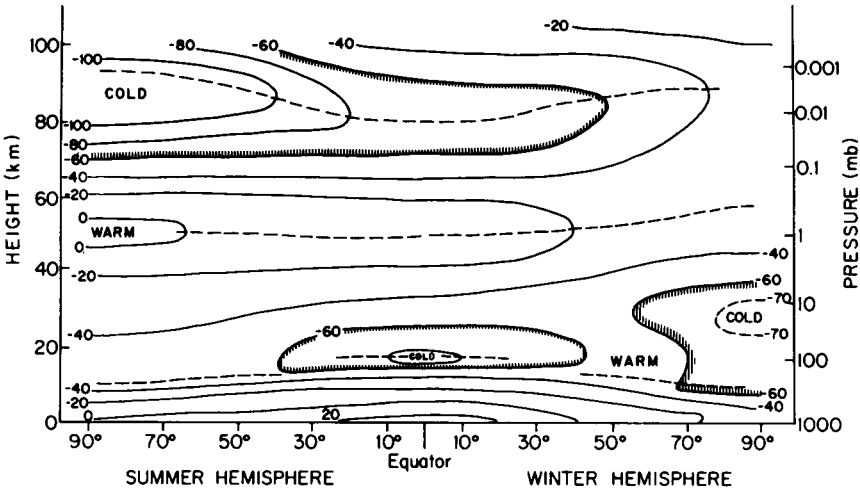

Fig. 1.3. Schematic latitude-height section of zonal mean temperatures (°C) for solstice conditions. Dashed lines indicate tropopause, stratopause, and mesopause levels. (Courtesy of R. J. Reed.)

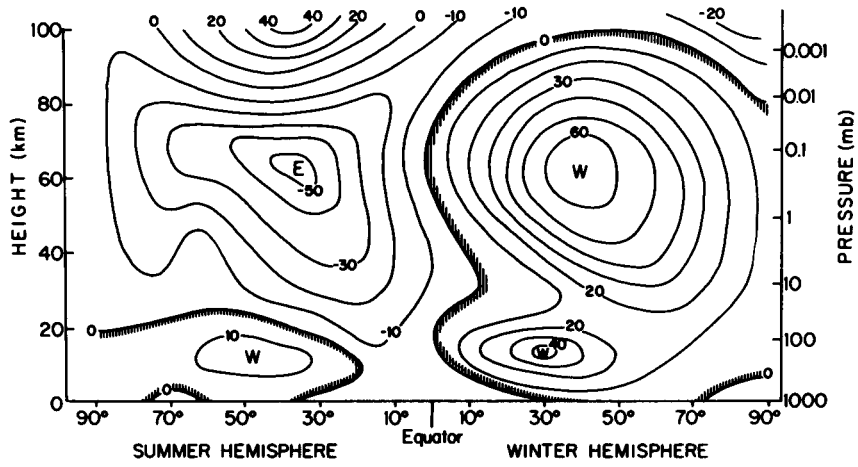

Fig. 1.4. Schematic latitude-height section of zonal mean zonal wind ($m\ s^{-1}$) for solstice conditions; W and E designate centers of westerly (from the west) and easterly (from the east) winds, respectively. (Courtesy of R. J. Reed.)

the lower stratosphere between the cold tropical tropopause and midlatitudes in the winter hemisphere, and the reversed temperature gradient above 60 km where temperatures increase uniformly from the summer pole to the winter pole. The summer polar mesopause is much colder than radiative equilibrium, while the winter polar temperatures are above radiative equilibrium throughout the entire middle atmosphere. Thus, dynamical processes must play an essential role in establishing the observed temperature and zonal wind distributions.

The cross sections of Figs. 1.3 and 1.4 should not be regarded as definitive climatologies. In reality there are substantial differences between the Northern and Southern Hemisphere solstice circulations (see Figs. 5.1 and 5.2). There is also a remarkable interannual variability in the middle atmosphere, especially in the winter hemisphere (see Chapter 12), so that many years of data are required to determine stable climatologies of the mean zonal wind and temperature distributions. Only in the past decade have adequate observations been available for the stratosphere, and for the mesosphere the data base is still unsatisfactory. However, the general features of the overall solstice circulation should be roughly as depicted in Figs. 1.3 and 1.4.

1.3 Composition of the Middle Atmosphere

In the lower and middle atmospheres, mixing by fluid motions on all scales tends to produce uniform mixing ratios for all gaseous constituents of the atmosphere. Only constituents with significant sources or sinks have spatially and temporally varying mixing ratios. For most such species the vertical variability is much greater than horizontal and temporal variability, so only vertical profiles are considered here. Horizontal and temporal variability are intimately related to dynamical transport processes. These will be discussed in Chapter 9.

The primary constituents in the lower and middle atmosphere are diatomic nitrogen and oxygen, which together account for 98.65% of the total mass of the dry atmosphere. The noble gas argon accounts for another 1.28%, so that the myriad of other species (often known as trace species) that have been detected in the atmosphere together account for less than 0.1% of the total mass. The primary constituents have no significant sources or sinks in the stratosphere or mesosphere, so that their mass fractions are nearly constant in height. In the thermosphere above 90 km the increasing molecular mean free paths lead to a gradual change from dominance of mixing by macroscopic fluid motions below 100 km to control by molecular diffusion above about 120 km. At altitudes where molecular diffusion dominates, each species (in the absence of sources or sinks) has an exponential

decay of density with height with a scale height determined by its molecular mass. Thus the less massive species increasingly dominate with height. The region of the atmosphere where eddy mixing dominates is referred to as the *homosphere*, while the molecular diffusion region is the *heterosphere*. These are separated by the *homopause*, near 110 km, which is often considered to be the level where the two processes are of equal importance.

1.3.1 Measures of Trace Constituent Concentration

Several different variables are used to describe the concentration of trace gases in the atmosphere. For example, the absolute concentration can be expressed in terms of the number of molecules per unit volume, n_T; the mass per unit volume, ρ_T; or the partial pressure, p_T. Note that

$$n_T M_T = \rho_T N_a, \qquad \text{and} \qquad n_A M_A = \rho_A N_a, \tag{1.3.1}$$

where N_a is Avogadro's number ($= 6.022 \times 10^{26}$ molecules kmol^{-1}), M stands for the molecular weight (kg kmol^{-1}), and the subscripts T and A stand for the trace constituent and "air" excluding the trace constituent, respectively. Since trace constituents in the middle atmosphere are present in such small quantities,

$$\rho_T \ll \rho_A \approx \rho, \qquad \text{and} \qquad p_T \ll p_A \approx p.$$

The partial pressure is related to the other concentration measures through the ideal gas law:

$$p_T = \rho_T R_* T / M_T, \qquad p = \rho R_* T / M_A, \tag{1.3.2a,b}$$

where R_* is the universal gas constant ($= 8.314 \times 10^3 \text{ J K}^{-1} \text{ kmol}^{-1}$) and where we have replaced p_A by p and ρ_A by ρ in Eq. (1.3.2b) with negligible error.

The number density, n_T, and the partial pressure, p_T, are often used for presentation of observational data. However, due to the compressibility of the atmosphere these are not conserved following the motion. For dynamical studies, *mixing ratio* is the preferred measure of concentration, since it is conserved following the motion in the absence of sources or sinks. Both *mass* mixing ratio (m) and *volume* mixing ratio (v; sometimes called the "mole fraction") are in common usage, although observational data are nearly always reported as volume mixing ratios. These are related to partial pressure as follows:

$$m = \rho_T / \rho = (p_T / p)(M_T / M_A), \tag{1.3.3a}$$

$$v = n_T / n_A = m(M_A / M_T) = p_T / p. \tag{1.3.3b}$$

Thus, $m \propto v = p_T/p$. Mass mixing ratios are usually used in thermodynamic and radiative transfer computations. Volume mixing ratios (or number densities) are essential in photochemical calculations involving the partitioning of molecules within groups. (For example, reactions involving conversions between O and O_3 conserve v but not m for the sum $O + O_3$.)

1.3.2 Major Trace Species

The radiatively active trace species water vapor, carbon dioxide, and ozone are the species of major importance for middle atmosphere dynamics. For convenience we refer to these collectively as "major" trace species. Of these three species only CO_2 is well mixed in most of the middle atmosphere, and even it has a detectable few percent decrease in fractional concentration with height due to the time lag in upward mixing of the CO_2 currently being produced by fossil fuel burning at the surface. In contrast, H_2O and O_3 are highly variable in space and time.

The variability of water vapor in the lower atmosphere is due entirely to the processes of evaporation, condensation, and sublimation that occur as part of the hydrological cycle. Although water vapor in the troposphere may have mixing ratios as high as 0.03 by volume, the stratosphere is observed to be extremely arid with mixing ratios in the range of 2–6 ppmv (parts per million by volume). The dryness of the stratosphere can be qualitatively accounted for if it is assumed that all air entering from the troposphere into the stratosphere passes through the extremely cold tropical tropopause (Fig. 1.3), where most of the remaining water content is frozen out. This "freeze-dry" model for the aridity of the stratosphere places important constraints on the nature of the mass exchange between the lower and middle atmosphere, as will be further discussed in Chapter 9. The extremely low water concentrations in the middle atmosphere make accurate measurement of the water vapor distribution very difficult. However, there is general agreement that the minimum concentration occurs in the lower stratosphere, with a gradual increase in the mixing ratio occurring above about 20 km due to the source provided by oxidation of methane. This type of profile is clearly shown in the water vapor measurements by the Limb Infrared Monitor of the Stratosphere (LIMS) satellite experiment (Fig. 1.5). Throughout the middle atmosphere the concentration of water vapor is too small for it to play much direct role in the local radiative heating or cooling. Radiatively, water vapor is important for the middle atmosphere primarily because the infrared emission by water vapor together with the vertical heat flux associated with convection are crucial for establishing the temperature

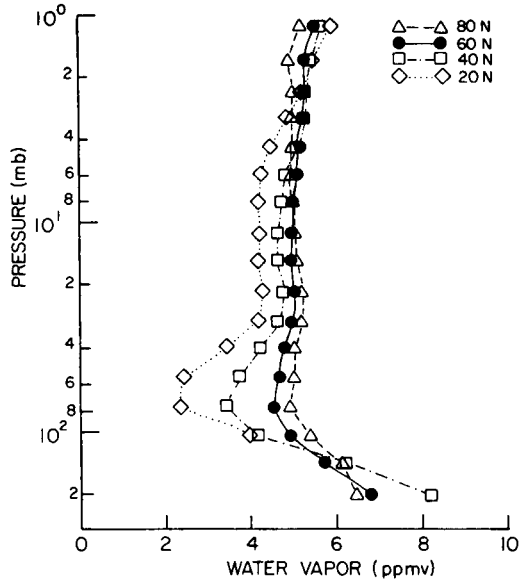

Fig. 1.5. Vertical profiles of water vapor mixing ratio at several latitudes measured by the LIMS instrument on the *Nimbus* 7 satellite for May 1-26, 1979. [From Remsberg *et al.* (1984b). American Meteorological Society.]

structure of the troposphere, and hence the temperature at the lower boundary of the middle atmosphere.

Ozone is, of course, the most significant trace species in the middle atmosphere. The absorption of solar ultraviolet insolation by ozone is the major radiative heat input for the middle atmosphere. By depleting the solar ultraviolet flux this absorption protects the biosphere from the damaging effects of ultraviolet radiation. The budget of atmospheric ozone, which involves very complex photochemical cycles depending on many trace species, both natural and manmade, is thus a major environmental concern. The observed spatial and temporal variability of many of the species involved in ozone photochemistry implies that transport and mixing by atmospheric motions are crucial aspects of the ozone problem. To a large extent it is the threat posed to the ozone layer by anthropogenic perturbations in atmospheric composition that has accounted for the rapid pace of middle atmospheric research in the past decade. The complex coupling among photochemical, radiative, and dynamical processes that ultimately controls the distribution of ozone still provides a major challenge for middle atmosphere research that will be discussed in Chapter 10.

The vertical profile of ozone for a midlatitude standard atmosphere is plotted in Figs. 1.6 and 1.7 in units of molecular concentration and mass

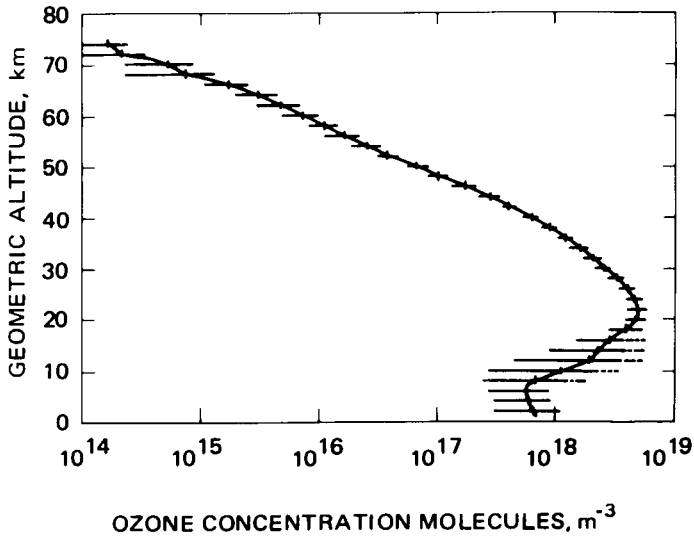

Fig. 1.6. Midlatitude standard ozone concentration profile (molecules m^{-3}). Horizontal bars show the standard deviation about the mean for observed profiles. [From the *U.S. Standard Atmosphere* (1976).]

mixing ratio, respectively. As Fig. 1.6 indicates, most of the mass of the ozone in the atmosphere is contained in the lower stratosphere with a maximum concentration near 22 km. However, the mixing ratio is a maximum at a much higher altitude (~37 km). Since most of the production of ozone molecules occurs above 30 km, the large molecular concentration below 30 km must result from downward transport by atmospheric motions. Thus, the observed ozone profile itself provides evidence of dynamical-chemical coupling. Despite its central role in the meteorology of the middle atmosphere, ozone is indeed a *trace* constituent. At the peak of the ozone layer the mixing ratio is only about 8–10 ppmv. If the entire column of ozone (i.e., the mass per unit area in a column of air extending from the surface to the top of the atmosphere) were brought to standard temperature and pressure (0°C, 1013.25 mb), the thickness of the column would only be about 3 mm!

1.3.3 Minor Trace Species

In addition to the three major radiatively active trace species, there are a large number of species present in sufficient concentrations to play significant roles in the chemistry of the middle atmosphere. We will refer

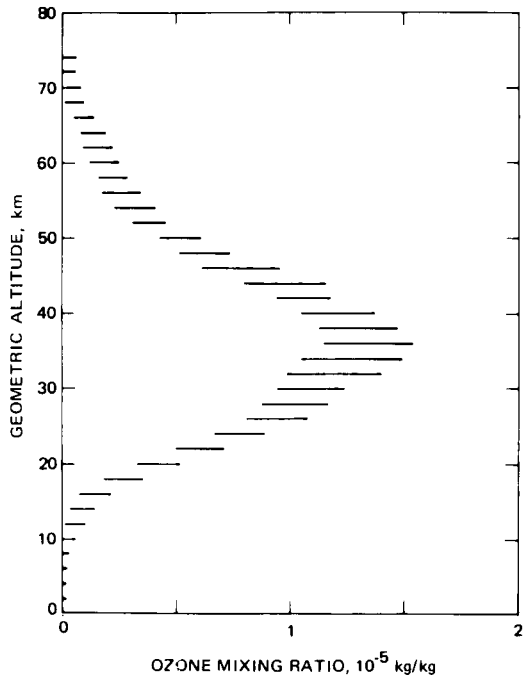

Fig. 1.7. The standard ozone profile of Fig. 1.6 plotted in terms of the mass mixing ratio. [From the *U.S. Standard Atmosphere* (1976).]

to these collectively as "minor" trace species. Of special significance for meteorological studies are the so-called "long-lived" trace species such as nitrous oxide (N_2O), methane (CH_4), and the chlorofluoromethanes (CF_2Cl_2 and $CFCl_3$). These species all have sources at the ground that are primarily natural for N_2O and CH_4 and entirely manmade for $CFCl_3$ and CF_2Cl_2. They are well mixed in the vertical in the troposphere and are destroyed in the stratosphere by oxidation and/or photodissociation. Thus, they all have vertical profiles in which mixing ratios decay with altitude in the middle atmosphere. Typical examples of midlatitude profiles for these tracers are shown in Fig. 1.8. The vertical gradient of mixing ratio varies enormously from the species with the slowest destruction rate in the stratosphere (CH_4) to the species with the most rapid destruction rate ($CFCl_3$). Such vertically stratified species provide excellent tracers for calibrating theoretical models of mass transport and diffusion in the middle atmosphere. Their observed meridional and temporal variability provide important clues as to the nature of transport and mixing by motion systems, as will be discussed in Chapter 9.

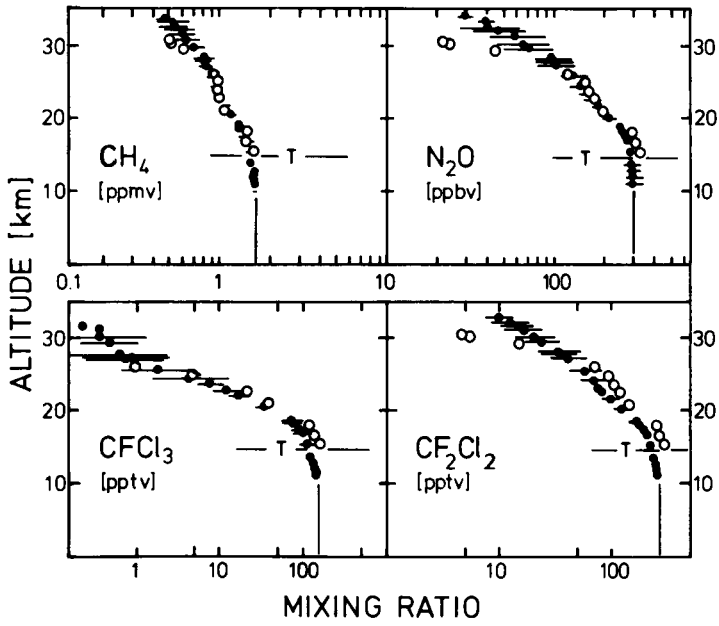

Fig. 1.8. Vertical volume mixing ratio profiles for several minor trace gases that have tropospheric sources and are photochemically destroyed in the stratosphere. All profiles are from balloon flights over Southern France (44°N). Full dots give average profiles for several summer flights. Open dots refer to a flight on October 21, 1982. [From Schmidt *et al.* (1984).]

1.4 The Vertical Distribution of Eddy Amplitudes

The observed longitudinally averaged zonal wind and temperature distributions in the middle atmosphere (Figs. 1.3 and 1.4) are maintained by the competing effects of differential radiative heating and the mechanical and thermal forcing by motions of all scales. Motions in the middle atmosphere occur on scales ranging from global-scale tides to microscale turbulent patches. Although turbulent mixing is thought to play a significant role in the momentum budget of the middle atmosphere, much of the momentum, heat, and tracer transport in the middle atmosphere is due to coherent wave motions of various classes. Discussion of such waves and their interactions with the mean flow will be a major theme of this book.

Wave motions in the atmosphere result from the competition between inertia and restoring forces acting on fluid parcels displaced from their equilibrium latitudes and/or elevations. For the waves of concern here, the restoring force is supplied either by gravity or by the poleward gradient of the planetary vorticity. The former is responsible for internal gravity waves (sometimes called buoyancy waves); the latter is responsible for Rossby

waves (often referred to as planetary waves). In addition there are mixed modes in which both types of restoring force play a role.

Both the gravity modes and the Rossby modes can be classified according to their horizontal structure, their vertical structure, and their sources of excitation. This classification scheme allows these waves to be categorized on the basis of the following dualities: (1) extratropical or global modes versus equatorially trapped modes, (2) vertically trapped (decaying) modes versus vertically propagating modes, and (3) free normal modes versus forced modes. (See Section 4.1 for further discussion.)

For the middle atmosphere, it is vertically propagating modes forced in the troposphere that are of primary importance, although forcing within the middle atmosphere is important for atmospheric tides (which may be regarded as gravity waves modified by rotation and compressibility). A qualitative indication of the variation of horizontal wind amplitude with

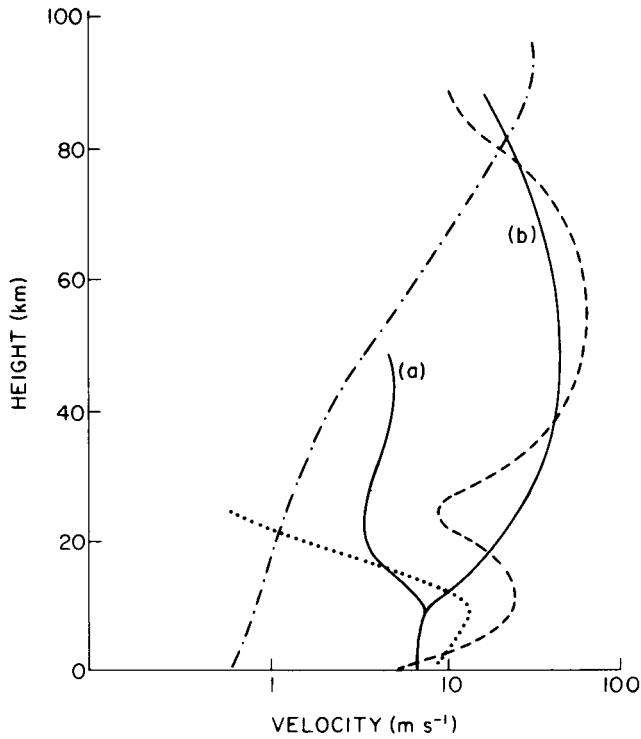

Fig. 1.9. Schematic vertical profiles of horizontal wind amplitudes corresponding to various types of atmospheric motions. Solid line: planetary waves (a) summer, (b) winter; dashed: zonal mean; dotted: synoptic scale; dotted-dashed: gravity waves. (Courtesy of Professor T. Matsuno.)

height for various types of motion is given in Fig. 1.9. Observations and theory (Section 4.5 and Chapter 5) indicate that the vertical structure of forced Rossby modes is critically dependent on their horizontal scale and on the mean zonal wind distribution. Synoptic-scale Rossby waves are strongly trapped in the troposphere and decay rapidly with height in the middle atmosphere, as indicated in Fig. 1.9. Planetary-scale Rossby waves, on the other hand, propagate vertically provided that their phase speeds are westward (but not too strongly westward) relative to the mean flow. Since the largest-amplitude planetary waves are stationary with respect to the ground, only in the winter hemisphere where the mean winds are westerly throughout the middle atmosphere are planetary wave amplitudes comparable to the magnitude of the mean zonal wind. In the summer hemisphere such waves cannot propagate past the level where the mean zonal flow vanishes, and hence are unable to penetrate beyond the lower stratosphere.

Nontidal gravity waves generated in the troposphere appear to have a rather broad two-dimensional spectrum of phase speeds that includes meridionally propagating modes as well as zonally propagating modes that are both westerly and easterly relative to the mean flow. Thus, during all seasons at least some gravity waves can propagate through the middle atmosphere without encountering critical levels at which the mean wind equals the phase speed. Observations indicate that in extratropical latitudes the vertical flux of gravity-wave activity is greater in the winter than in the summer. This seasonal dependence is probably due primarily to variations in the strength of tropospheric sources. In addition, there is an important seasonal dependence of the phase speed spectrum due to selective transmission caused by the presence of mean wind critical levels. During the summer (winter), waves that are easterly (westerly) relative to the mean flow are selectively filtered out so that there is a net upward transfer of westerly (easterly) momentum (see Sections 4.6.2 and 7.3).

Gravity-wave modes with sufficiently high Doppler-shifted frequencies will tend to propagate through the stratosphere without significant damping, so that energy density remains approximately constant in height and the horizontal velocity amplitude increases as the inverse square root of density, $\rho_0^{-1/2}$. Thus, although gravity waves (and atmospheric tides) contribute only a small part of the eddy horizontal wind variance in the troposphere and stratosphere, in the upper mesosphere they often appear to be the dominant modes. At some level in the mesosphere or lower thermosphere the amplitudes may become so great that such waves break down due to convective overturning or shear instability. Above 100 km, molecular diffusion becomes increasingly important in limiting wave amplitudes.

The vertical distribution of turbulence is very poorly known. However, since most turbulence in the middle atmosphere appears to result from

gravity-wave breakdown, it is likely that the vertical profile of the wind variance due to turbulent motions is similar to that due to gravity waves.

1.5 Observational Techniques

Although observations of the stratosphere date from as early as 1902, when the French scientist Teisserenc de Bort discovered the stratosphere by means of balloon temperature soundings (see Hartmann, 1985, for a discussion), systematic observation of the middle atmosphere dates only from the International Geophysical Year (IGY) of 1957–1958. Knowledge concerning the temperatures, winds, and composition of the middle atmosphere has increased dramatically in the years following the IGY.

During the 1960s the operational meteorological radiosonde network provided sufficiently frequent soundings of the lower stratosphere up to about the 10-mb level so that the climatology of the lower stratosphere gradually was established at least in the Northern Hemisphere. In the same period a meteorological rocket network was established that provided wind and temperature measurements in the upper stratosphere and lower mesosphere. A network of balloon-borne ozonesondes was also operated for a relatively brief time. These *in situ* measurement techniques were only deployed at a limited number of locations (primarily the North American region) and could not provide global climatologies.

Observation of the global stratosphere really only began in 1969 with the launching of the *Nimbus* 3 satellite. This research satellite and subsequent research and operational satellites have provided more than a decade of global remote sounding of stratospheric temperatures and total ozone as well as limited measurements of profiles of ozone and a few other trace constituents.

Satellite temperature soundings generally are based on measurements of the infrared emission in the 15-μm band of carbon dioxide. Such measurements are done on an operational basis using nadir-viewing instruments. However, the vertical resolution of these devices is quite low, since they measure characteristic temperatures in layers 10–15 km deep (see Fig. 2.36). Limb-sounding radiometers [such as the LIMS and Stratospheric and Mesospheric Sounder (SAMS) instruments on *Nimbus* 7) are able to provide much better vertical resolution (approximately 3–5 km) in the middle atmosphere, since most of the signal is returned from the altitude at which the instrument scans the limb of the atmosphere (see Fig. 2.38).

Infrared emission instruments are not easily used for detecting minor trace species because of the low ratio of signal to noise. An alternative technique useful in some cases is the solar occultation method, in which

the absorption of gas (or aerosol extinction) is measured by viewing the sun on the limb near sunrise or sunset (see Fig. 2.39). Good vertical resolution and high signal-to-noise ratios are possible, but the technique obviously can provide only limited latitudinal and diurnal coverage. Ozone has been measured using solar and stellar occultation, but the primary satellite observations of ozone are based either on infrared emission in the 9.6-μm band or on the backscatter of ultraviolet sunlight. The latter method is, of course, limited to sunlit regions.

Satellite remote observations to date have provided only temperature and constituent measurements. Horizontal winds have been deduced from temperature fields, using the thermal wind relationship to build upward from operational height analyses for some base level (e.g., 100 mb). The accuracy of such geostrophic winds is thus dependent on the base-level analyses, which may have substantial errors in data sparse regions.

Direct velocity measurements in the middle atmosphere have been made *in situ* by rocket soundings and remotely from the ground using several radar methods, operating in a variety of frequency ranges. These include the partial reflection drift method, meteor radars, and so-called MST (mesosphere–stratosphere–troposphere) radars. In the partial reflection drift technique, a triangular array of receivers is used to determine the drift velocities of ionized irregularities that partially reflect the radar signal. Only bulk horizontal motions can be sensed with this technique, and measurements are limited to the middle and upper mesosphere and lower thermosphere. Meteor radars are Doppler radars that measure line of sight velocities using returns from ionized meteor trials in the mesopause region. The MST technique utilizes very-high-frequency (VHF) radars (wavelengths of the order of a few meters) in Doppler mode to determine the drift velocities of back-scattering elements whose nature depends on the region being scanned. The echoes received by such radars from the troposphere and lower stratosphere are caused by refractive-index variations due to density fluctuations associated with neutral atmosphere (clear air) turbulence. In the mesosphere the echoes are produced by scattering due to fluctuations in free electron density associated with turbulence. With the MST technique it is possible to obtain three-dimensional velocity fields. MST radars have limited horizontal coverage but can produce data with high temporal and vertical resolution in a given locality. They are thus particularly appropriate for studying high-frequency components of the motion field, such as gravity waves and tides.

MST radars cannot provide information on the temperature fluctuations associated with atmospheric motions. Such information can be provided by ground-based lidar sounding. Lidars designed to detect the Rayleigh back-scatter from air molecules can yield density profiles in the altitude

range of 30–90 km. From these the temperature profile can be computed using Eqs. (1.1.1) and (1.1.2). Other types of lidars can be used to provide profiles of ozone, aerosols, and other trace constituents in the middle atmosphere.

References

1.1. Atmospheric statics is discussed in more detail in standard meteorological texts such as Holton (1979a) and Wallace and Hobbs (1977).

1.3. *U.S. Standard Atmosphere, 1976* provides much useful information on the structure and composition of the atmosphere.

1.5. Remote sounding techniques are discussed in depth by Houghton *et al.* (1984). Gage and Balsley (1984) present a review of recent advances in remote sensing and provide an extensive bibliography of papers on both passive and active techniques.